First Principles Study of Electronic Band Structure and Structural Stability of Al_2C Monolayer and Nanotubes

S Pramchu, A P Jaroenjittichai, and Y Laosiritaworn

Department of Physics and Materials Science, Faculty of Science, Chiang Mai University, Chiang Mai, Thailand
Thailand Center of Excellence in Physics, Commission on Higher Education, Bangkok, Thailand.

The corresponding author's e-mail: yongyut_laosiritaworn@yahoo.com

Abstract. We used density functional theory (DFT) based on generalized gradient approximation (GGA) and hybrid functional (HSE06) to investigate band gap and structural stability of Al_2C monolayer and nanotubes. From the results, both GGA and HSE06 band gaps of Al_2C monolayer agree well with previously reported data. For the Al_2C nanotubes, we found that their band gaps are more sensitive to the size and the chirality than that of the widely studied SiC_2 nanotubes, indicating the Al_2C nanotubes may have higher band gap tuning capabilities (with varying diameter size and chirality) compared with those of SiC_2 nanotubes. We have also discovered a desirable direct band gap in the case of (n,0) nanotubes, although Al_2C monolayer band gap is indirect. The calculated strain energy reveals that (n,0) nanotubes constructed by wrapping up Al_2C monolayer consume less energy than (0,n) nanotubes. Thus, (n,0) nanotubes is easier to synthesize than (0,n) nanotubes. This discovery of direct band gap in (n,0) Al_2C nanotubes and their adjustable band gap suggests them as promising sensitizer for enhancing power conversion efficiency of excitonic solar cells.

1. Introduction

Excitonic solar cells (XSC) based on heterojunction nanostructure composed of low-dimensional materials have gained a great deal of interest due to its large interface area and high efficiency in generating excitons [1-3]. In general, the power conversion efficiency (PCE) of this XSC depends strongly on the interface band alignment between donor and acceptor materials [4]. Therefore, low-dimensional materials with tunable band alignment are highly desirable for achieving high PCE. One of the most efficient methods used in experimental laboratory to tune desirable property is to change materials morphology. For instance, different morphologies, e.g., thin film, nanosheet, and nanotube usually possess different properties. In addition, the difference in diameter and chirality of nanotube can generally lead to a variety of materials properties [5, 6].

Several low-dimensional materials have been suggested as suitable candidate for XSC application. A honeycomb BeN_2 sheet has high carrier mobility but its band gap of 2.23 eV is quite large for solar cell application [7]. SiC_2 siligraphene (g-SiC_2) with a direct band gap of 1.09 eV attracts more attention than BeN_2 nanosheet but its nanotube band gaps are reported independent of the chirality and diameter (with diameters > 8.0 Å) [8, 9]. Therefore, it is difficult to tune SiC_2 nanotube band gaps by

varying its chirality and diameter. Among many candidates, Al_2C monolayer with band gap of 1.05 eV has been also proposed as a suitable material for photovoltaic applications [10, 11]. However, the dependence on chirality and diameter of its nanotube - electronic band structure is yet to report.

Therefore, in this work, we sought for the possibility to tune the Al_2C band gap by varying nanotube radius and chirality. We performed DFT calculation based on GGA and HSE06 (as used in Ref. [7-11]) to investigate band gap and structural stability of Al_2C in low-dimensional structures, with a focus on nanotube structure. The dependence on chirality and diameter of Al_2C nanotube band gaps calculated in this work is expected to suggest which chirality and diameter is appropriate to yield the desirable band gap for high power conversion efficiency in XSC application.

2. Materials and Methods

Structural information of Al_2C monolayer, i.e. lattice parameters and atomic positions reported in Ref. [11], was used as an initial structure for our DFT structural relaxation. The relaxed Al_2C monolayer is with band gap of 1.05 eV and has planar tetracoordinate carbons, bonding to four Al atoms in the same plane (as shown in **Fig. 1(a)**). This relaxed Al_2C monolayer was then used to perform electronic band structure calculation.

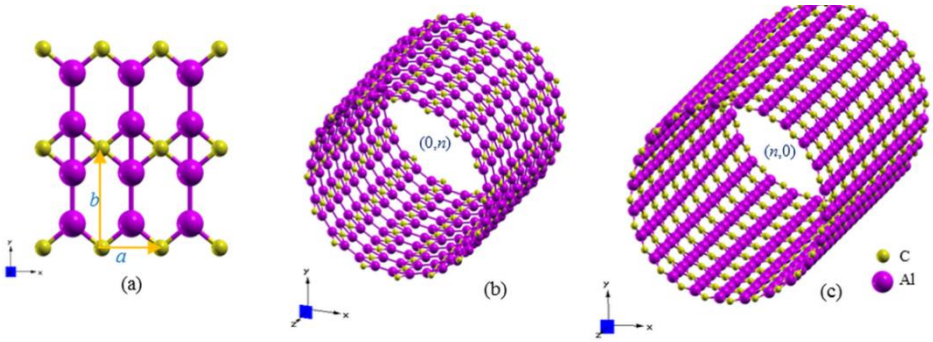

Figure 1. The structures of Al_2C, (a) Al_2C monolayer, (b) (0,16) nanotube, and (c) (24,0) nanotube.

Also, as shown in **Fig. 1(b,c)**, the nanotubes were constructed by wrapping a monolayer of Al_2C into a seamless cylinders. Generally, a pair of indices (n,m) is usually used to define the way the monolayer is wrapped. For Al_2C nanotubes, the integers n and m denote the number of unit vector along the direction of lattice vectors a and b (see **Fig. 1 (a)**), respectively. Thus, several nanotube structures are possible to get constructed. In this work, we focused on (n,0) and (0,n) nanotubes as a prototype study. The chirality of (n,0) and (0,n) nanotubes considered via nanotube-axis can be simply classified as vectors along b-axis and a-axis, respectively. To analyse structural stability of nanotubes, we need to calculate strain energy (E_s) which for the case of nanotube it could be defined as $E_s = (1/N_{NT})E_{NT} - (1/N_{ML})E_{ML}$ [9], where E_{NT}, E_{ML}, N_{NT}, and N_{ML} denote total energies and number of atoms of the considered nanotube (NT) and monolayer (ML) supercell, respectively.

In the DFT calculation, the calculation were performed under the framework of the plane wave method implemented in Quantum-Espresso package [12], where electron-ion interactions are described by norm-conserving pseudopotentials [13, 14]. In the considered system, valence states included the Al 3s and 3p states; and C 2s and 2p states. The generalized gradient approximation (GGA) with parameters obtained from Perdew-Burke-Ernzerhoff approach (PBE) [15] was used. The energy cutoff of 80 and 320 Rydberg were found sufficiently large for wavefunction and charge density expansions, respectively. The k-point mesh with 12×12×1 and 1×1×12 Monkhorst-Pack grid [16] was employed in the calculations of Al_2C monolayer and nanotubes, respectively.

For electronic band structure calculation, the Heyd-Scuseria-Ernzerhof (HSE) screened hybrid density functional [17] has been also used to calculate band structures of compounds with the relaxed structures acquired from GGA. The Heyd-Scuseria-Ernzerhof (HSE) screened hybrid density functional with 25% portion of exact-exchange is suitable and usually used for band structure

calculation of these 1D and 2D materials [8, 10, 11]. Thus, these parameter settings have been used throughout this work.

3. Results and Discussions

Our predicted lattice constant *a*, obtained using GGA, is similar to the GGA results reported in Ref. [11]. Specifically, we predicted that a = 3.04 Å while Ref. [11] reported a = 3.03 Å. For lattice constant *b*, our calculation yields b = 5.60 Å, which is equal to the result from Ref. [10, 11]. Also, we found that Al_2C monolayer exhibits band structure with indirect band gap, where VBM and CBM located at S and Y high-symmetry points, respectively (as shown in **Fig. 2(a)**). Our calculated indirect (S → Y) and direct (Y → Y) band gaps obtained using HSE06 hybrid functional are 1.03 and 1.25 eV, respectively, while the HSE06 indirect and direct band gap reported in Ref. [11] are 1.05 and 1.25 eV, respectively. The slight difference (1.9%) in our calculated indirect band gap compared with that from Ref. [11] may be caused by the slight discrepancy (about 0.3%) in lattice constant, *a*. The difference between calculation methods used in this work and those in Ref. [11] is we employed norm-conserving pseudopotential but Ref. [11] used projector-augmented wave (PAW). This probably leads to the slight discrepancy in results. However, our calculations for lattice constants and band gaps still yield good agreement with the reference results. This indicates that our calculations for structural relaxation and band structure are reliable and can be applied for Al_2C nanotubes.

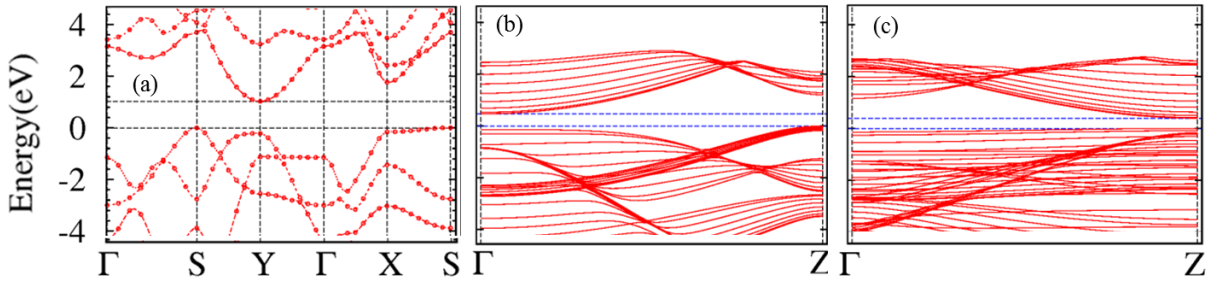

Figure 2. Band structures of Al_2C monolayer and nanotubes, i.e. (a) HSE06 results for Al_2C monolayer, (b) GGA results for (0,16) nanotube, and (c) GGA results for (24,0) nanotube. "Z" point is defined at (0.0, 0.0, 0.5) crystal coordinate of the nanotube structure.

As is seen in **Fig. 2(b,c)**, (0,16) nanotube exhibits band structure with indirect band gap (Z → Γ) while (24,0) nanotube displays direct band gap at Z point. We also used GGA to calculate band structures of (*n*,0) and (0,*n*) nanotubes with diameter varied from 6 Å to 27 Å. Although GGA usually underestimates band gap [7-11], our HSE06 hybrid functional calculations for band gaps of (0,16) and (24,0) nanotubes indicate that the direct and indirect band character is not different from those of GGA results (this trend was also found in Refs. [7-11]). Our calculated HSE06 band gaps for (0,16) and (24,0) nanotubes are 1.08 eV (indirect) and 0.95 eV (direct), respectively. Although Al_2C monolayer exhibits indirect band characteristic, we found that band gaps of (*n*,0) nanotubes with $n \leq 28$ are all direct bands. With the direct band gap, electrons and holes can directly transfer between VBM and CBM without any change in their momenta. Further, strain energy shown in **Fig. 3(a)** indicates that (*n*,0) nanotubes constructed by wrapping up a Al_2C monolayer into a tube consume less energy than that of the (0,*n*) nanotubes (for all *n* shown in **Fig. 3(a)**). This suggests that (*n*,0) nanotubes are easier to synthesize than (0,*n*) nanotubes. **Fig. 3(a)** also reveals that (*n*,0) nanotubes are more stable than (0,*n*) nanotubes with the same diameter because of their lower total energies per atom extracted from the definition of E_s ($E_s = (1/N_{NT})E_{NT} - (1/N_{ML})E_{ML}$). Note that (*n*,0) and (0,*n*) nanotubes have the same empirical formula (i.e. Al_2C), the structural stability between these nanotubes can then be directly compared via their total energies per atom.

From **Fig. 3(b)**, for the (0,*n*) nanotubes, band gap increases with decreasing diameter. In addition, our calculations predict that the band gap of (*n*,0) nanotube vanishes (i.e. the metallic state) when nanotube diameter (*d*) is reduced to about 8.0 Å. **Figure 3(b)** also displays the trend that band gaps of

both (0,*n*) and (*n*,0) nanotubes can be tuned to that of monolayer when the diameter is sufficiently large (> 27 Å for Al_2C nanotube). These size and chirality dependences of Al_2C nanotube band gaps are similar to the case of SiC_2 siligraphene [8] but band gaps of Al_2C nanotubes are more sensitive to the size and chirality. This is because Al_2C has larger unit cell compared with that of SiC_2, and the nanotube with larger unit cell is generally more sensitive to the variation of nanotube curvature.

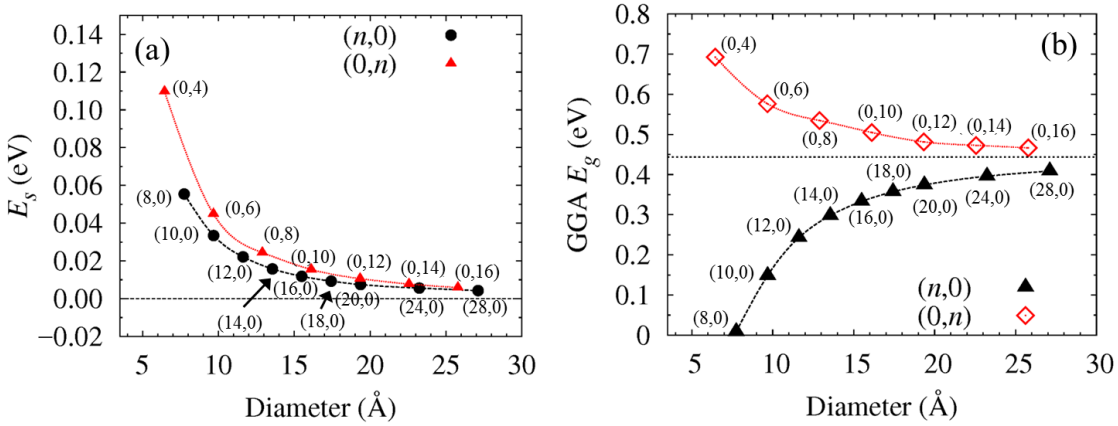

Figure 3. (a) Strain energy (E_s) and (b) GGA band gap (E_g) as a function of nanotube diameter and chirality. (0,*n*) and (*n*,0) denote chirality with tube axis aligned along vector *a* and *b*, respectively.

4. Conclusion

In this work, electronic band structure and strain energy of (0,*n*) and (*n*,0) Al_2C nanotubes have been investigated. We found that (*n*,0) Al_2C nanotubes with $n \leq 28$ exhibit direct band gap, although the band gap of Al_2C monolayer is indirect. The desirable direct band gap was then discovered in the case of (*n*,0) nanotubes, which is suitable for solar cell applications. The calculated strain energy also reveals that it is easier to synthesize the (*n*,0) nanotubes than the (0,*n*) ones. In addition, we found that band gap of Al_2C nanotubes are somewhat sensitive to the diameter size and chirality. This indicates that it is possible to tune the band gap of Al_2C nanotubes by varying their diameter size and chirality. These (*n*,0) Al_2C nanotubes with direct and tuneable band gap exhibit their capability to be utilized as efficient materials in enhancing the power conversion efficiency of excitonic solar cells.

References

[1] Yu K and Chen J 2009 *Nanoscale Res. Lett.* **4** 1-10
[2] Gregg B A 2003 *J. Phys. Chem. B* **107** 4688-4698
[3] Semonin O E, Luther J M and Beard M C 2012 *Mater. Today* **15** 508-515
[4] Meng L, You J, Guo T-F and Yang Y 2016 *Acc. Chem. Res.* **49** 155-165
[5] Bauer S, Pittrof A, Tsuchiya H and Schmuki P 2011 *Electrochem. Commun.* **13** 538-541
[6] Grace T, Yu L, Gibson C, Tune D, Alturaif H, Al Othman Z and Shapter J 2016 *Nanomater.* **6** 52
[7] Zhang C and Sun Q 2016 *J. Phys. Chem. Lett.* **7** 2664-2670
[8] Zhou L-J, Zhang Y-F and Wu L-M 2013 *Nano Lett.* **13** 5431-5436
[9] Li Y, Li F, Zhou Z and Chen Z 2011 *J. Am. Chem. Soc.* **133** 900-908
[10] Li Y, Liao Y, Schleyer P v R and Chen Z 2014 *Nanoscale* **6** 10784-10791
[11] Dai J, Wu X, Yang J and Zeng X C 2014 *J. Phys. Chem. Lett.* **5** 2058-2065
[12] Limbach H J, Arnold A, Mann B A and Holm C 2006 *Comput. Phys. Commun.* **174** 704-727
[13] Hamann D R 1989 *Phys. Rev. B* **40** 2980-2987
[14] Troullier N and Martins J L 1991 *Phys. Rev. B* **43** 1993-2006
[15] Perdew J P, Burke K and Ernzerhof M 1996 *Phys. Rev. Lett.* **77** 3865-3868
[16] Monkhorst H J and Pack J D 1976 *Phys. Rev. B* **13** 5188-5192
[17] Aliaksandr V K, Oleg A V, Artur F I and Gustavo E S 2006 *J. Chem. Phys.* **125** 224106